Butyrate Improves Insulin Sensitivity and Increases Energy Expenditure in Mice

Zhanguo Gao,[1] Jun Yin,[1] Jin Zhang,[1] Robert E. Ward,[2] Roy J. Martin,[1] Michael Lefevre,[2] William T. Cefalu,[1] and Jianping Ye[1]

OBJECTIVE—We examined the role of butyric acid, a short-chain fatty acid formed by fermentation in the large intestine, in the regulation of insulin sensitivity in mice fed a high-fat diet.

RESEARCH DESIGN AND METHODS—In dietary-obese C57BL/6J mice, sodium butyrate was administrated through diet supplementation at 5% wt/wt in the high-fat diet. Insulin sensitivity was examined with insulin tolerance testing and homeostasis model assessment for insulin resistance. Energy metabolism was monitored in a metabolic chamber. Mitochondrial function was investigated in brown adipocytes and skeletal muscle in the mice.

RESULTS—On the high-fat diet, supplementation of butyrate prevented development of insulin resistance and obesity in C57BL/6 mice. Fasting blood glucose, fasting insulin, and insulin tolerance were all preserved in the treated mice. Body fat content was maintained at 10% without a reduction in food intake. Adaptive thermogenesis and fatty acid oxidation were enhanced. An increase in mitochondrial function and biogenesis was observed in skeletal muscle and brown fat. The type I fiber was enriched in skeletal muscle. Peroxisome proliferator–activated receptor-γ coactivator-1α expression was elevated at mRNA and protein levels. AMP kinase and p38 activities were elevated. In the obese mice, supplementation of butyrate led to an increase in insulin sensitivity and a reduction in adiposity.

CONCLUSIONS—Dietary supplementation of butyrate can prevent and treat diet-induced insulin resistance in mouse. The mechanism of butyrate action is related to promotion of energy expenditure and induction of mitochondria function. ***Diabetes*** **58:1509–1517, 2009**

Recent studies suggest that natural compounds represent a rich source for small thermogenic molecules, which hold potential in the prevention and treatment of obesity and insulin resistance. Several natural products, such as resveratrol (1,2), bile acid (3), and genipin (4), have been reported to increase thermogenic activities in animal or cellular models. In the current study, we provide evidence for the thermogenic activity and therapeutic value of a short-chain fatty acid, butyric acid, in a mouse model of metabolic syndrome. Butyric acid has four carbons in the molecule ($CH_3CH_2CH_2$-COOH) and becomes sodium butyrate after receiving sodium. Sodium butyrate is a dietary component found in foods such as cheese and butter. It is also produced in large amounts from dietary fiber after fermentation in the large intestine, where butyric acid is generated together with other short-chain fatty acids from nondigestible carbohydrates, such as nonstarch polysaccharides, resistant starch, and miscellaneous low-digestible saccharides (5,6). The bioactivities of sodium butyrate are related to inhibition of class I and class II histone deacetylases (7). Histone deacetylases regulate gene transcription through modification of chromatin structure by deacetylation of proteins, including histone proteins and transcription factors. To our knowledge, there is no report about butyrate in the regulation of insulin sensitivity or energy metabolism.

Dietary intervention is a potential strategy in the prevention and treatment of metabolic syndrome. Peroxisome proliferator–activated receptor (PPAR)-γ coactivator (PGC)-1α, a transcription coactivator, is a promising molecular target in dietary intervention (1,2). PGC-1α controls energy metabolism by interaction with several transcription factors, e.g., estrogen-related receptor-α, nuclear respiratory factor-1 and -2, PPAR-α and -δ, and thyroid hormone receptor, that direct gene transcription for mitochondrial biogenesis and respiration (8). In the muscle, PGC-1α increases oxidative (type I) fiber differentiation and enhances fatty acid metabolism (9). In brown fat, PGC-1α stimulates adaptive thermogenesis through upregulation of uncoupling protein (UCP)-1 expression (10). A reduction in PGC-1α function is associated with mitochondrial dysfunction, reduction in fatty acid oxidation, and risk for insulin resistance or type 2 diabetes (11–14). Dietary intervention of PGC-1α activity holds promise in the prevention and treatment of metabolic syndrome. However, our knowledge is limited in the dietary components or derivatives that are able to regulate the PGC-1 activity. In the current report, we provide evidence that sodium butyrate induced PGC-1 activity in skeletal muscle and brown fat in mice.

RESEARCH DESIGN AND METHODS

Male C57BL/6J (4 weeks old) mice were purchased from the Jackson Laboratory (Bar Harbor, ME). After 1 week quarantine, the C57BL/6J mice were fed a high-fat diet (D12331; Research Diets, New Brunswick, NJ), in which 58% of calories is from fat. All of the mice were housed in the animal facility with a 12-h light/dark cycle and constant temperature (22–24°C). The mice had free access to water and diet. All procedures were performed in accordance with National Institutes of Health guidelines for the care and use of animals and were approved by the institutional animal care and use committee at the Pennington Biomedical Research Center.

Sodium butyrate administration. Sodium butyrate (303410; Sigma) was incorporated into the high-fat diet at 5% wt/wt. Sodium butyrate was blended into the diet using a food processor at 400 rpm. The sodium butyrate–

From the [1]Antioxidant and Gene Regulation Laboratory, Pennington Biomedical Research Center, Louisiana State University System, Baton Rouge, Louisiana; and [2]Nutrition and Food Sciences, Utah State University, Logan, Utah.

Corresponding author: Jianping Ye, yej@pbrc.edu.

Received 24 November 2008 and accepted 24 March 2009.

Published ahead of print at http://diabetes.diabetesjournals.org on 14 April 2009. DOI: 10.2337/db08-1637.

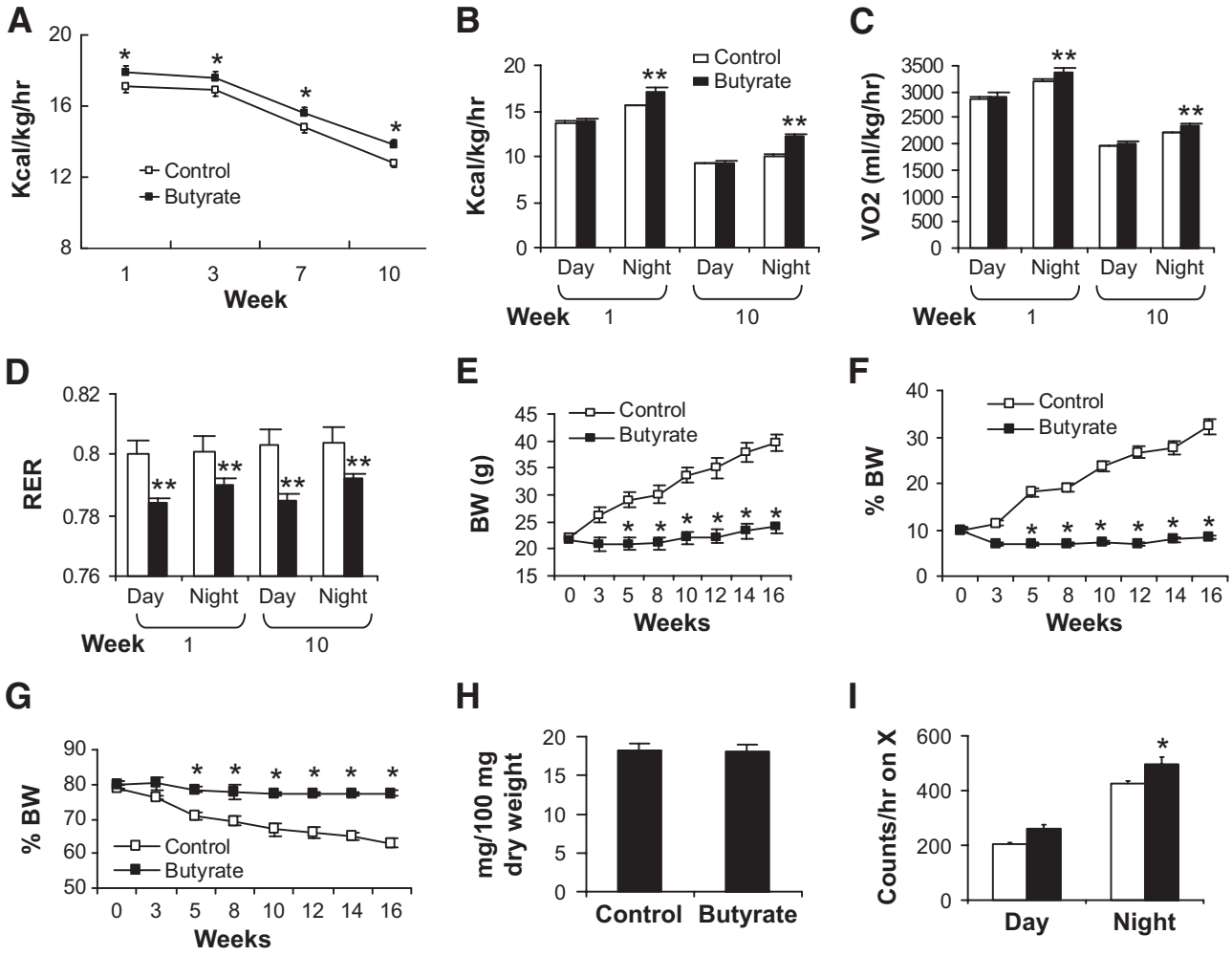

FIG. 1. Energy metabolism in response to sodium butyrate. Butyrate increased energy expenditure in C57BL/B6 mice. Energy expenditure was examined using the metabolic chamber at the 1st week and the 10th week on high-fat diet (16 weeks in age). In this study, sodium butyrate was used at 5% wt/wt in high-fat diet. *A*: Food intake. Food intake was monitored daily for 5 days at each time point. Average daily food intake (g) was converted into kilocalories and normalized with body weight (kg) and 24 h. *B*: Energy expenditure measured as kilocalories per kilogram lean mass per hour. *C*: Oxygen consumption measured as milliliters volume oxygen per kilogram lean mass per hour. *D*: Substrate utilization. This is expressed by respiratory exchange ratio (RER), which is the volume ratio of oxygen consumed versus CO_2 exhaled. *E*: Body weight (BW). *F*: Body fat content in percentage of body weight. This was determined by nuclear magnetic resonance. *G*: Body muscle content in percentage of body weight. *H*: Lipid in feces. Feces were collected in the cages during a 24-h period on high-fat diet at 12 weeks. Total lipids were extracted and quantified ($P > 0.05$, $n = 5$). *I*: Spontaneous physical activity. The frequency of horizontal movement (X) was shown for day and night at 10 weeks on a high-fat diet. For *A–D*, and *I*, $n = 8$ in the control or butyrate group. For *E–G*, $n = 10$ in the control or butyrate group. Values are the means ± SE. *$P < 0.05$, **$P < 0.001$ by Student's *t* test. □, Control; ■, butyrate.

containing diet was pelleted and stored in a –20°C freezer until usage. On the supplemented diet, mice could receive sodium butyrate at $5\ g \cdot kg^{-1} \cdot day^{-1}$ at the normal daily rate of calorie intake.

Intraperitoneal insulin tolerance. Intraperitoneal insulin tolerance testing was conducted by intraperitoneal injection of insulin (I9278; Sigma) at 0.75 units/kg body wt in mice after a 4-h fast, as described previously (15).

Nuclear magnetic resonance. Body composition was measured for the fat content using quantitative nuclear magnetic resonance as previously described (15).

Quantitative real-time RT-PCR. Total RNA was extracted from frozen tissues (kept at −80°C) using Tri-Reagent (T9424; Sigma), as described previously (16). TaqMan RT-PCR primer and probe were used to determine mRNA for PGC-1α (Mm00447183_m1), UCP-1 (Mm00494069_m1), PPAR-δ (Mm01305434_m1), and carnitine palmitoyltransferase-1b (CPT1b; Mm00487200_m1). The reagents were purchased from Applied Biosystems (Foster City, CA). Mouse ribosomal 18S rRNA_s1 (without intron-exon junction) was used as an internal control. The reaction was conducted with a 7900 HT Fast real-time PCR system (Applied Biosystems).

Metabolic chamber. Energy expenditure, respiratory exchange ratio, spontaneous physical movement, and food intake were measured simultaneously for each mouse with a comprehensive laboratory animal monitoring system (Columbus Instruments, Columbus, OH) as described previously (15).

Body temperature in cold response. Body temperature was measured in the cold room with ambient temperature at 4°C. Animals were sedated and restrained for <30 s during the measurement. A Thermalert model TH-8 temperature monitor (Physitemp, Clifton, NJ) was used with the probe placed in the rectum at 2.5 cm in depth.

Western blotting. Fresh fat and muscles were collected and frozen immediately in liquid nitrogen. The whole-cell lysate was prepared in a lysis buffer with sonication as described previously (16). Antibodies and their sources are myoglobin (sc-25607; Santa Cruz Biotechnology), phosphorylated Akt (threonine 308 [Thr308], no. 9275; Cell Signaling), tubulin (ab7291; Abcam), phosphorylated insulin receptor substrate-1 (tyrosine 632 [Tyr632], no. sc-17196; Santa Cruz Biotechnology), myosin (M8421; Sigma), phosphorylated AMP kinase (AMPK; Thr172, no. 2531; Cell Signaling), and pP38 (sc-7975; Santa Cruz Biotechnology). The antibodies to PGC-1α and UCP-1 were from Dr. Thomas Gettys at our institute (Pennington Biomedical Research Center).

Muscle fiber type. The fiber types in skeletal muscle were examined using two methods: succinate dehydrogenase staining for ATPase and immunostaining of type I myosin heavy chain. In the succinate dehydrogenase staining, midbelly cross-sections of muscle were cut at 8 μm in a cryostat (–20°C). After drying for 5 min at room temperature, the sections were incubated at 37°C for 60 min in incubation solution containing 6.5 mmol/l sodium phosphate

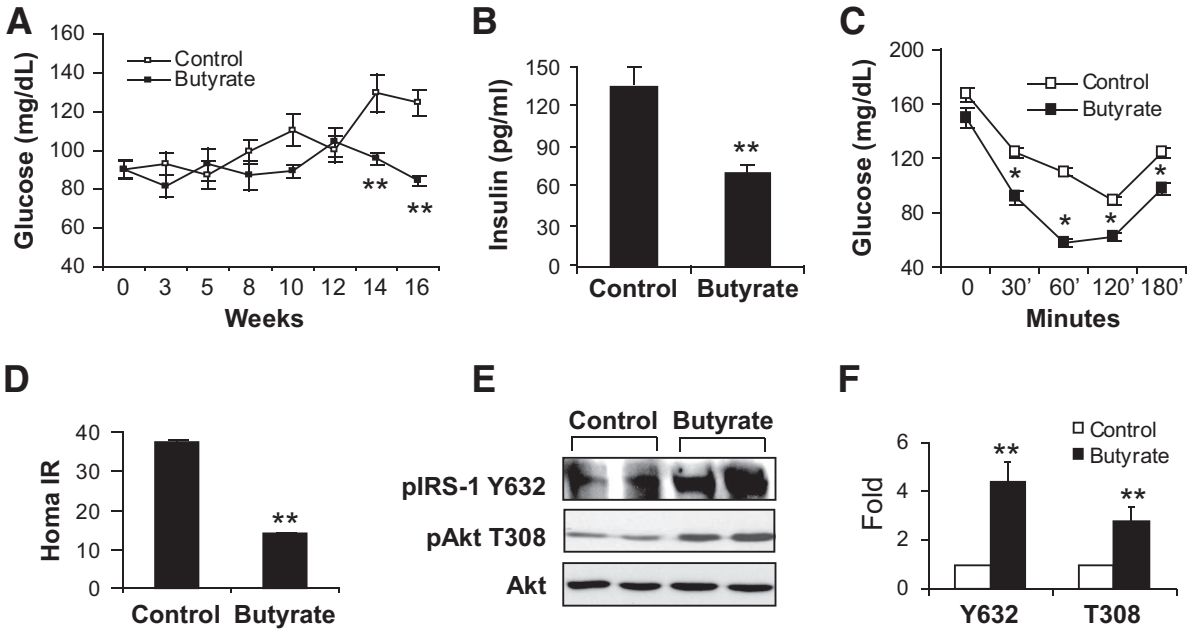

FIG. 2. Insulin sensitivity in butyrate-treated mice. *A*: Fasting glucose. Tail vein blood was used for glucose assay after 16 h fasting during the period of high-fat diet feeding. *B*: Fasting insulin. The insulin level was determined at 16 weeks on high-fat diet in fasting condition with a Lincoplex kit (MADPK model). *C*: Intraperitoneal insulin tolerance in butyrate-treated mice. Intraperitoneal insulin tolerance testing was performed at 12 weeks on high-fat diet (at 16 weeks of age). In *A–C*, data are the means ± SE (n = 9). *P < 0.05, **P < 0.001 by Student's t test. *D*: HOMA-IR. After an overnight fast, blood glucose and insulin were measured and used to determine insulin sensitivity through HOMA-IR (IR = fasting insulin mU/ml × fasting glucose mg/dl ÷ 405). Values are the means ± SE (n = 8 mice). **P < 0.001. *E*: Insulin signaling. The gastrocnemius muscle was isolated after insulin (0.75 units/kg) injection in mice for 30 min and used to prepare the whole-cell lysate for immunoblot. The mice on high-fat diet for 13 weeks were used in the signaling assay. *F*: Signal quantification. The blot signal in *E* was quantified and presented after normalization with protein loading. **P < 0.001 (n = 2). IRS, insulin receptor substrate.

monobasic, 43.5 mmol/l sodium phosphate biphasic, 0.6 mmol/l nitroblue tetrazolium (74032; Sigma), and 50 mmol/l sodium succinate (14160; Sigma). The sections were rinsed three times (30 s each time) in 0.9% saline, 5 min in 15% ethanol, and then mounted with aqueous mounting medium (DakoCytomation).

Immunohistostaining. Fresh skeletal muscle was collected, embedded in gum tragacanth mixed with OCT freezing matrix, and quickly frozen in liquid nitrogen. The tissue slides were obtained through serial cross-section cutting at 8 μm thickness. The slide was blotted with type I myosin heavy-chain antibody (M8421; Sigma) at 1:200 dilution. After being washed, the slide was incubated with a biotinylated secondary antibody (BA-2000), and the color reaction was performed using ABC elite reagent (PK-6101). A 3,3′-diaminobenzidine substrate kit (SK-4100) was used to obtain signal for myosin I.

Hematoxylin and eosin staining. Fresh tissues (brown adipose tissue [BAT]) were collected at 16 weeks of age after 12 weeks on the sodium butyrate–containing diet. Tissue was fixed in 10% formalin solution (HT50–1-2; Sigma). Tissue slides were obtained through serial cross-section cutting 8 μm in thickness and processed with standard procedure.

Histone deacetylase assay and nuclear extract preparation. Histone deacetylase assay was conducted using a histone deacetylase assay kit (17-320; Upstate). Briefly, the muscle nuclear extract (10 μg) was incubated with [^{3}H]acetyl CoA (TRK688; Amersham) radio-labeled histone H4 peptide (25,000 cpm, as a substrate) at 37°C for 12 h by shaking. Released [^{3}H]acetate was measured using a scintillation counter. The nuclear extract was prepared according to a protocol described previously (17).

Lipids in serum and feces. The serum fatty acids, including butyrate, were examined using a protocol described elsewhere (18). The detail is presented in Supplement 1, available in an online appendix at http://diabetes.diabetesjournals.org/cgi/content/full/db08-1637/DC1. Fatty acids in feces were determined using the protocol from a study by Schwarz et al. (19). Triglyceride and cholesterol were measured in whole blood with a Cardiochek portable test system.

Statistical analysis. Data are the means ± SE from multiple samples. All of the in vitro experiments were conducted at least three times. Student's t test or two-way ANOVA was used in the statistical analysis with significance set at $P \leq 0.05$.

RESULTS

Energy metabolism. We first tested butyrate in prevention of dietary obesity. In the diet-induced obesity model, butyrate supplementation started at the beginning of high-fat diet feeding. Plain high-fat diet was used in the control group. Calorie intake was monitored four times in the first 10 weeks. After normalization with body weight, calorie intake was reduced with the increase in age. In the butyrate group, it was significantly higher at all of the time points (Fig. 1*A*). Energy expenditure, oxygen consumption, and substrate utilization were monitored using a metabolic chamber. In the butyrate group, energy expenditure and oxygen consumption were elevated at night (Fig. 1*B* and *C*). The respiratory exchange ratio was reduced during the day and night (Fig. 1*D*), suggesting an increase in fatty acid oxidation in response to butyrate. These data suggest that sodium butyrate may increase energy expenditure in the diet-induced obesity model.

Body weight and fat content were monitored in this study. In the control mice, body weight increased from 23 to 40 g after 16 weeks on high-fat diet (Fig. 1*E*), and fat content (adiposity) increased from 10 to 35% of body weight (Fig. 1*F*). Accordingly, lean mass was reduced from 80 to 65% (Fig. 1*G*). In the butyrate group, these parameters were not significantly changed during the 16 weeks on high-fat diet (Fig. 1*E*, *F*, and *G*), suggesting that butyrate prevented diet-induced obesity. Mouse growth was not influenced by butyrate because body length was identical between the two groups. Dietary fat digestion and absorption in the gastrointestinal tract was examined by measuring fatty acid content in feces. Fat content was identical in the feces of the two groups (Fig. 1*H*), suggesting that

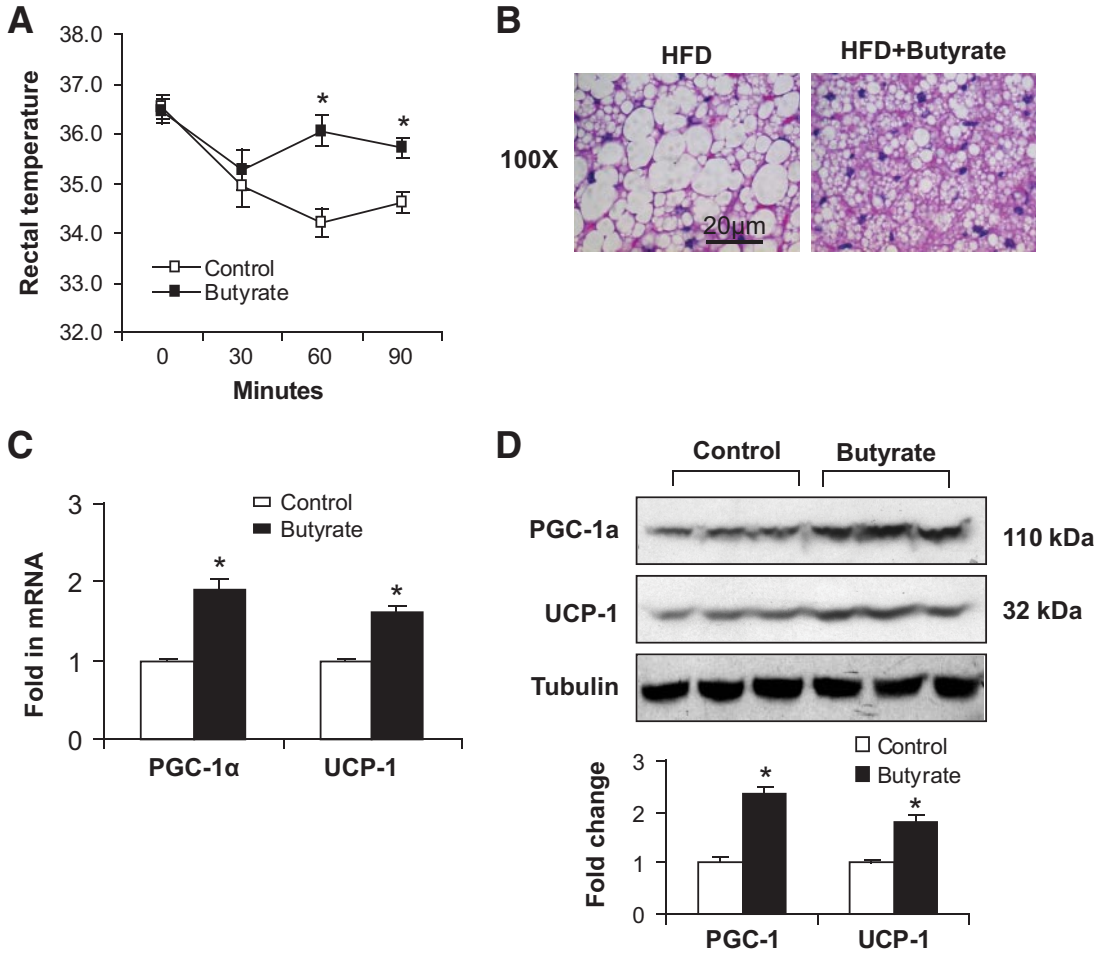

FIG. 3. Brown adipose tissue response to sodium butyrate. *A*: Adaptive thermogenesis in cold environment. Rectum temperature was measured when the mice were exposed to 4°C ambient temperature in a cold room at 10 weeks on high-fat diet. Details of the procedure are described in RESEARCH DESIGN AND METHODS. *B*: Hematoxylin and eosin staining in BAT. The staining was conducted in BAT collected at 13 weeks on high-fat diet. Photograph was taken at ×100 magnification. *C*: mRNA expression in BAT. BAT was collected at 13 weeks on high-fat diet. Gene expression was examined by qRT-PCR. mRNA of PGC-1α and UCP-1 in brown fat of mice treated with butyrate was measured. *D*: Immunoblot of protein in BAT. BAT was collected at 13 weeks of butyrate treatment. The whole-cell lysate (100 μg) was resolved in SDS-PAGE and blotted with PGC-1α and UCP-1 antibodies. Data are the means ± SE (n = 9 mice). *P < 0.05. (A high-quality digital representation of this figure is available in the online issue.)

butyrate does not influence fat absorption by the gastrointestinal tract. Spontaneous physical activity was monitored during the day and night in the mice. The data suggest that physical activity was not reduced by butyrate (Fig. 1*I*). Increased activity was observed in the butyrate group at night. These data suggest that dietary supplementation with butyrate protected the mice from diet-induced obesity. This effect is associated with an increase in energy expenditure and fatty acid oxidation. The food intake and physical activity suggests that no toxicity was observed for butyrate in the mice.

Insulin sensitivity. The increase in energy metabolism suggests that butyrate may protect mice from high-fat diet–induced insulin resistance. To test this possibility, systemic insulin sensitivity was analyzed by fasting glucose, fasting insulin, and insulin tolerance. In the control group, fasting glucose was increased significantly after 10 weeks on high-fat diet (Fig. 2*A*). In the butyrate group, this increase was not observed (Fig. 2*A*). Fasting insulin was 50% lower in the butyrate group at 16 weeks on high-fat diet (Fig. 2*B*). In the intraperitoneal insulin tolerance test, the butyrate group exhibited much better response to insulin at all time points (30, 60, 120, and 180 min) (Fig. 2*C*). Homeostasis model assessment for insulin resistance (HOMA-IR) was 60% lower in the butyrate group (Fig. 2*D*). These data suggest that insulin resistance was prevented in the butyrate group. Insulin signaling was examined in the skeletal muscle lysate with Tyr632 (Y632) phosphorylation of insulin receptor substrate-1 protein and Thr308 phosphorylation of Akt (Fig. 2*E*). Both signals were increased in the butyrate-treated mice (Fig. 2*E* and *F*), suggesting a molecular mechanism of insulin sensitization.

BAT. The association of increased food intake with elevated energy expenditure led us to study BAT, which is responsible for adaptive thermogenesis in response to diet or cold (20–22). Diet-induced thermogenesis reduces obesity in both humans and animals (23). In the butyrate group, the increase in energy expenditure was observed at night when mice actively took food (Fig. 1*A* and *B*). This result suggests an increase in thermogenesis. To determine the thermogenic function, we conducted a cold-response experiment. Mice were exposed to a cold environment with an ambient temperature of 4°C for 90 min. Core body temperature was monitored three times by measuring the rectal temperature. In control mice, body

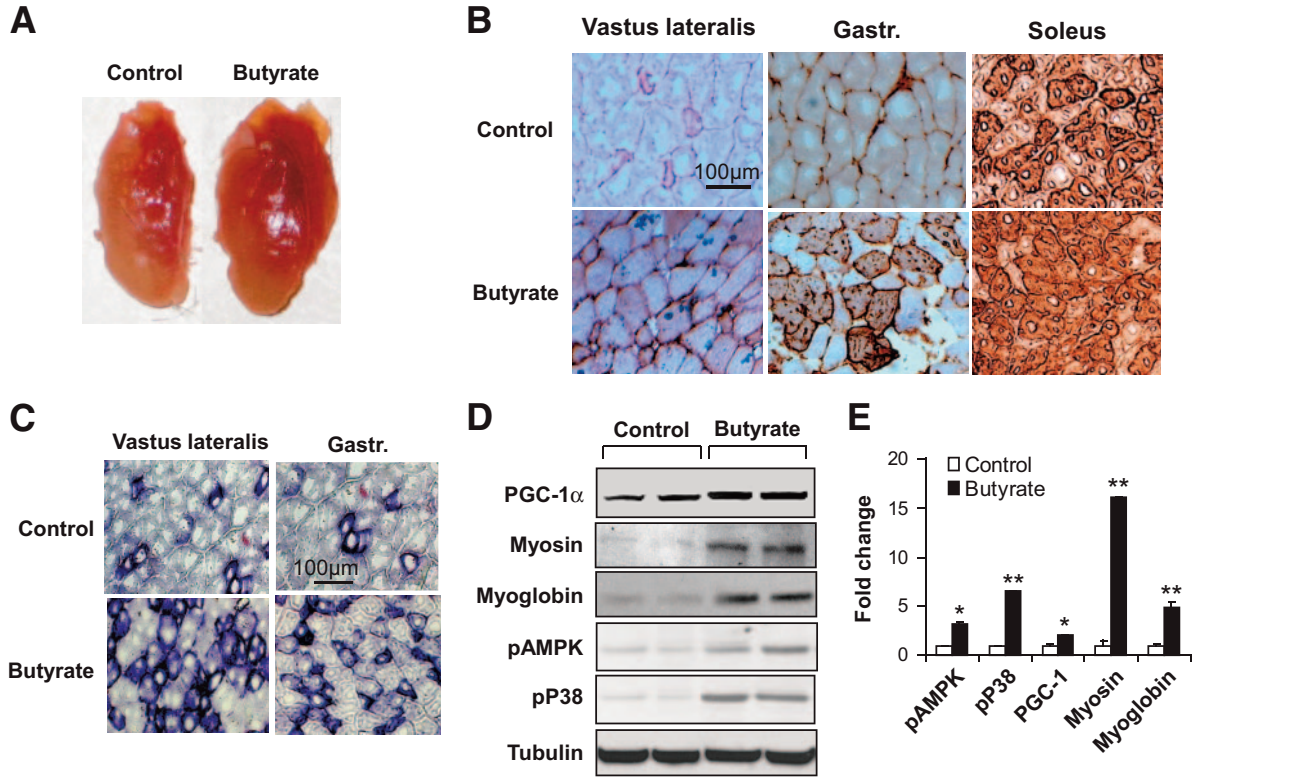

FIG. 4. Oxidative fiber in skeletal muscle. *A*: Vastus lateralis muscle. The tissue was isolated from mice that were fed high-fat diet for 13 weeks. *B*: Oxidative fiber (type I fibers) in serial cryostat sections of muscle. The muscle tissue slides were made from vastus lateralis, gastrocnemius (gastr.), and soleus muscle. They were stained with antibody against type I myosin heavy chain for oxidative fibers, as indicated by the brown color. The photograph was taken at ×20 magnification. *C*: Succinate dehydrogenase staining of oxidative fibers. The oxidative fibers were stained in serial cryostat sections of the vastus lateralis and gastrocnemius (gastr.) muscle as indicated by dark blue color in the photomicrograph. *D* and *E*: Quantification of proteins in immunoblot. The whole-cell lysate was prepared from muscle tissues and analyzed in an immunoblot. Signals for PGC-1α, type I myosin heavy chain, myoglobin, phosphorylated AMPK (pAMPK), and phosphorylated p38 (pP38) were blotted with specific antibodies. A representative blot is shown. Relative signal strength was quantified for each band and expressed in the bar figure. Results are the means ± SE (n = 8 mice). *P < 0.01, **P < 0.001 (vs. control). (A high-quality digital representation of this figure is available in the online issue.)

temperature decreased with time and was 34.5°C after 90 min in the cold (Fig. 3*A*). In butyrate-treated mice, body temperature dropped to 35°C transiently at 30 min and then returned to 36°C for the remainder of the time. These data suggest that thermogenic function is enhanced in the butyrate group.

Brown fat is critical for adaptive thermogenesis in mice. Morphology and gene expression were examined in brown fat. Compared with the control mice, the size of brown adipocytes was much smaller in the butyrate group (Fig. 3*B*), suggesting higher thermogenic activity that leads to the reduction in fat accumulation. Mitochondrial function is regulated by gene expression (24). To understand the molecular basis of the increased thermogenesis, we examined the expression of two thermogenesis-related genes, PGC-1α and UCP-1, in BAT. mRNA of both genes was increased in the butyrate-treated mice (Fig. 3*C*). The increase was observed in their proteins in the brown fat (Fig. 3*D*). The increased gene expression provides a molecular basis for enhanced thermogenesis by butyrate treatment.

Skeletal muscle. To understand the cellular basis of enhanced fatty acid utilization in the butyrate group, we assessed muscle fiber types. PGC-1α was reported to induce transformation of skeletal muscle fiber from glycolytic type (type II) into oxidative type (type I) in transgenic mice (9). Type I fibers are distinct from type II fibers in several properties (25). Type I fibers (oxidative and slow-twitch fibers) are rich in mitochondria, red in color, and active in fat oxidation for ATP biosynthesis. Type II fibers (glycolytic and fast-twitch fibers) are relatively poor in mitochondrial activity, lighter in color, and dependent on glycolysis in ATP production. The butyrate effect on PGC-1α in BAT suggests that skeletal muscle fibers may be changed by butyrate.

Compared with the control group, the butyrate group exhibited a deep red color (Fig. 4*A*). Fiber type analysis was conducted in the vastus lateralis, gastrocnemius (rich in glycolytic fibers), and soleus (rich in oxidative fiber). Type I fiber was determined with type I myosin heavy-chain immunohistostaining. The ratio of type I fibers were increased in all of the skeletal muscles of butyrate-treated mice (Fig. 4*B*). The increase was confirmed with a metachromatic dye–ATPase assay, in which the type I fibers were blue in color (Fig. 4*C*). To support the change in muscle morphology, the proteins of type 1 myosin heavy chain and PGC-1α were quantified in muscle lysate in an immunoblot. A significant increase was observed in both proteins in butyrate-treated mice (Fig. 4*D*). Myoglobin (another marker of oxidative type I fiber) was also increased by butyrate (Fig. 4*D*). A mean value of each protein is presented in Fig. 4*D*. These data suggest that the ratio of type I fiber was increased by butyrate in skeletal muscle.

AMPK and p38 activities were examined by their phosphorylation status. Their activities may contribute to elevation of PGC-1α protein through enhanced protein stability (26–28). It was not clear whether this mechanism was activated by butyrate. To test this possibility, we examined activity of AMPK and p38 in skeletal muscle. An

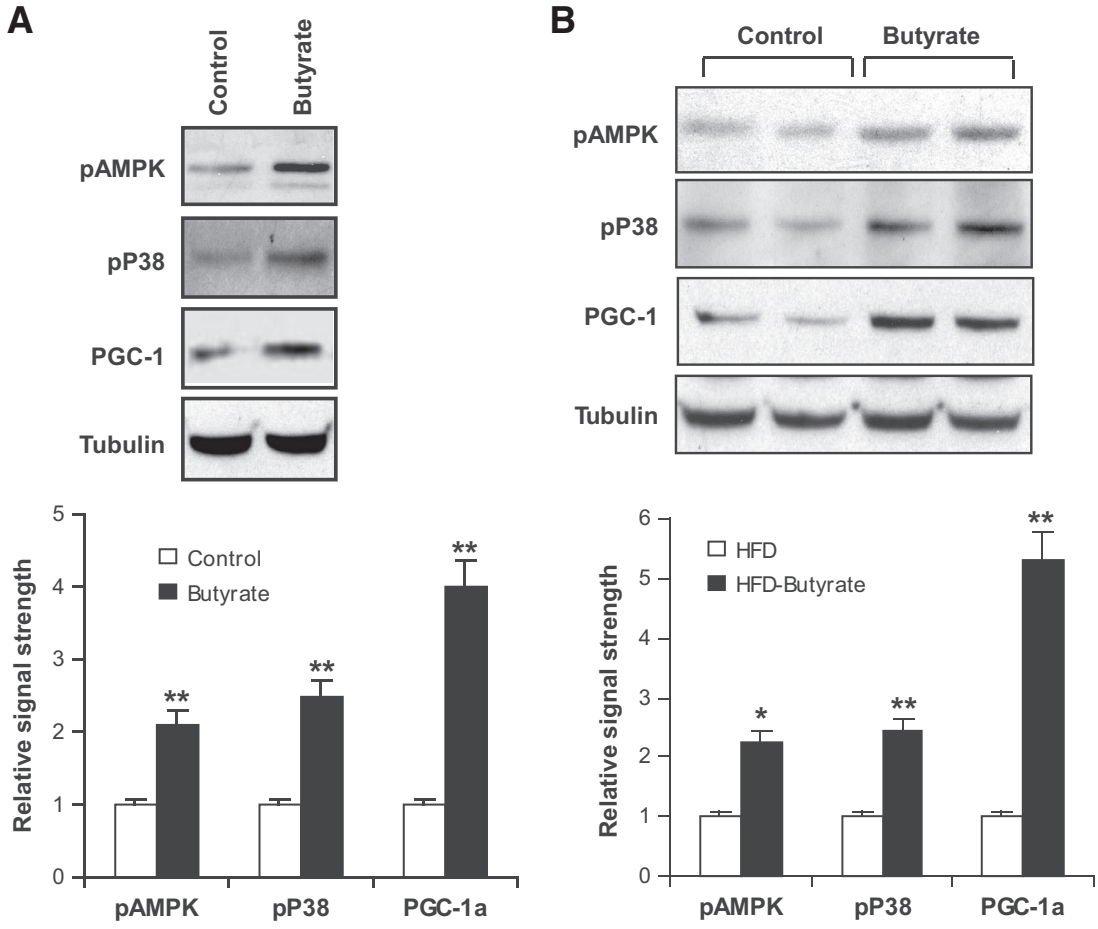

FIG. 5. Effect of butyrate on L6 muscle cells and liver tissues. *A*: AMPK and PGC-1α in L6 cells. Differentiated L6 myotubes were starved in 0.25% BSA and Dulbecco's modified Eagle's medium overnight. The cells were treated with 500 μmol/l of sodium butyrate for 4 h and analyzed in an immunoblot. A mean value of triplicate experiments is shown in the bar figure. *B*: AMPK and PGC-1α in liver. The whole-cell lysate was prepared from liver tissues collected from mice on high-fat diet (HFD) for 13 weeks and analyzed in an immunoblot. In the experiments, phosphorylated AMP kinase (pAMPK), phosphorylated p38 (pP38), and PGC-1α were blotted with the specific antibodies. A representative blot is shown. A mean value of five mice is shown in the bar figure ($n = 5$). *$P < 0.05$; **$P < 0.001$.

increase in their phosphorylation was observed in muscle lysate of butyrate-treated mice (Fig. 4*D*), suggesting increased activation of the two kinases by butyrate. In the L6 cell line, AMPK and p38 phosphorylation was increased by butyrate in the cell culture (Fig. 5*A*), suggesting butyrate is able to activate AMPK directly. In the same culture, PGC-1α protein was increased (Fig. 5*A*). In the liver of butyrate-treated mice, a similar pattern of changes was observed in AMPK, p38, and PGC-1α (Fig. 5*B*). These data consistently suggest that AMPK and p38 were activated by butyrate and that their activation may contribute to the increase in PGC-1α activity.

Mitochondrial function. Mitochondrial function was examined in skeletal muscle tissue and L6 muscle cells under butyrate treatment. Fatty acid oxidation was monitored in gastrocnemius muscle with ^{14}C-labeled palmitic acid. A 200% increase in ^{14}C-labeled CO_2 was observed in butyrate-treated mice (Fig. 6*A*). Fatty acid oxidation was associated with expression of PGC-1α target genes, such as CPT1b and COX-I (cytochrome c oxidase I) (9). Expression of these two genes was increased in skeletal muscle of butyrate-treated mice (Fig. 6*B* and *C*). The nuclear receptor PPAR-δ promotes fatty acid oxidation in skeletal muscle (29). PPAR-δ expression was also increased in butyrate-treated mice (Fig. 6*B*). In cultured L6 cells, a similar increase was observed in fatty acid oxidation and gene expression after butyrate treatment (Fig. 6*D* and *E*). These data consistently support the role of butyrate activity in the promotion of mitochondrial function.

Histone deacetylase activity in muscle. The butyrate concentration was analyzed in serum collected from the butyrate and control groups. In the fasted condition (overnight fast), the butyrate concentration was 7.23 ± 0.93 μg/ml in the butyrate group and 5.71 ± 0.38 μg/ml in the control animals. In the fed condition, the butyrate concentration was 9.40 ± 1.36 μg/ml in the butyrate group versus 5.48 ± 0.60 μg/ml in the control mice ($P < 0.05$, $n = 5$) (Fig. 6*F*). The data suggest that dietary supplementation increased butyrate levels in the blood. It is likely that the metabolic activity of butyrate is related to inhibition of histone deacetylase. Sodium butyrate inhibits the class I and class II histone deacetylases. To test this possibility, histone deacetylase activity was examined in skeletal muscle of mice at 16 weeks on high-fat diet (Fig. 6*F*). The assay was conducted with nuclear extracts of muscle samples. Histone deacetylase activity was reduced by 50% in the butyrate group (Fig. 6*G*). Trichostatin A (TSA), a typical histone deacetylase inhibitor, was used as a positive control in the parallel treatment. Histone deacetylase activity was decreased in the skeletal muscle of TSA-treated mice (Supplement 2). These data suggested that dietary supplementation of butyrate leads to suppression

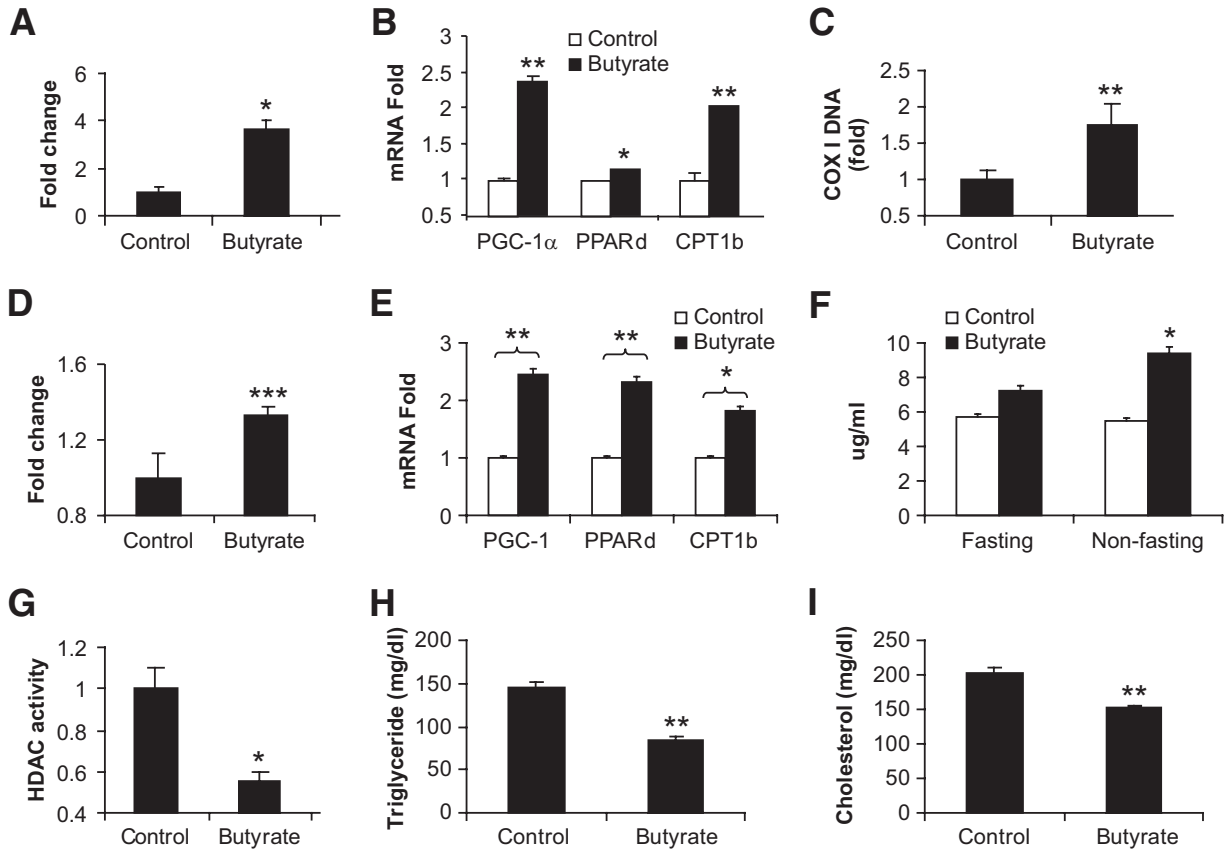

FIG. 6. Mitochondrial function and blood lipids. Vastus lateralis muscle and blood samples were collected from mice at 13 weeks on high-fat diet (18 weeks in age) and examined for fatty acid oxidation, gene expression, and blood lipids. *A*: Fatty acid oxidation in muscle. The *y*-axis represents fold change in ^{14}C-labled CO_2. *B*: Gene expression in muscle. Relative fold change in mRNA was used to indicate gene expression. *C*: Mitochondrial DNA COX-I (cytochrome c oxidase I) determined by SYBR Green RT-PCR. *D*: Fatty acid oxidation in L6 cells. Fully differentiated L6 cells were treated with 500 μmol/l butyrate for 16 h, and fatty acid oxidation was measured. *E*: Gene expression in L6 cells. Relative fold change in mRNA was used to indicate gene expression. *F*: Butyrate in serum. *G*: Histone deacetylase activity in muscle. *H*: Triglyceride in blood. *I*: Total cholesterol in blood. Data are the means ± SE (n = 6). *$P < 0.05$; **$P < 0.001$.

of histone deacetylase activity in the body. Total triglyceride and cholesterol were examined in the blood. These lipids were reduced in the butyrate group (Fig. 6*H* and *I*).

Treatment of obesity with butyrate. In the prevention studies, butyrate was administrated together with high-fat diet during the induction of obesity. To test butyrate in the treatment of obesity and insulin resistance, we administrated butyrate to obese mice that had been on a high-fat diet for 16 weeks. After a 5-week treatment with butyrate, the obese mice lost 10.2% of their original body weight, which dropped from 37.6 to 34.4 g (Fig. 7*A*). In the control group, body weight increased by 15.8% (from 35.9 to 41.6 g) during the same time period. Consistent with the change in body weight, fat content was reduced by 10% in the butyrate group (Fig. 7*B*). Furthermore, fasting glucose was reduced by 30% from 131 to 98.6 mg/dl ($P < 0.016$), HOMA-IR was reduced by 50%, and intraperitoneal insulin tolerance was improved significantly in the butyrate group (Fig. 7*C* and *D*). These data suggest that butyrate is effective in the treatment of obesity and insulin resistance in the dietary obese model.

DISCUSSION

Metabolic activities of butyric acid were examined in this study in diet-induced obese mice. The most important observation is that butyrate supplementation at 5% wt/wt in high-fat diet prevented development of dietary obesity and insulin resistance. It also reduced obesity and insulin resistance in obese mice. In butyrate-treated mice, the plasma butyrate concentration was increased, and blood lipids (triglycerides, cholesterol, and total fatty acids) were decreased (Fig. 6*H–I* and Supplement 1). The change in insulin sensitivity may be a consequence of a reduction in adiposity in our model. The increase in energy expenditure and fatty acid oxidation may be responsible for the antiobesity effect of butyrate. Butyrate supplementation did not reduce food intake, fat absorption, or locomotor activity, suggesting that there was no toxicity from butyrate. Butyrate was tested at 5 and 2.5% wt/wt in the high-fat diet in this study. At the lower (2.5% wt/wt) dosage, similar metabolic activity was observed (Supplement 3). At 5% in the high-fat diet, butyrate increased the calorie content from 58 to 64.4% in the fat. The increase in fat calories may not contribute to our observation of the antiobesity activity for butyrate. A recent study of weight-loss diets suggests that total calorie intake, not diet composition, is responsible for weight reduction in humans (30). At the cellular level, butyrate increased mitochondrial respiration, as indicated by the increase in oxygen consumption and CO_2 production. At the molecular level, increased expression of PGC-1α, PPAR-δ, and CPT1b may be involved in the stimulation of mitochondrial function by butyrate.

The current study indicates that in vivo butyrate is a novel activator of PGC-1α. PGC-1α activity may be regulated by butyrate at three levels. PGC-1α expression was

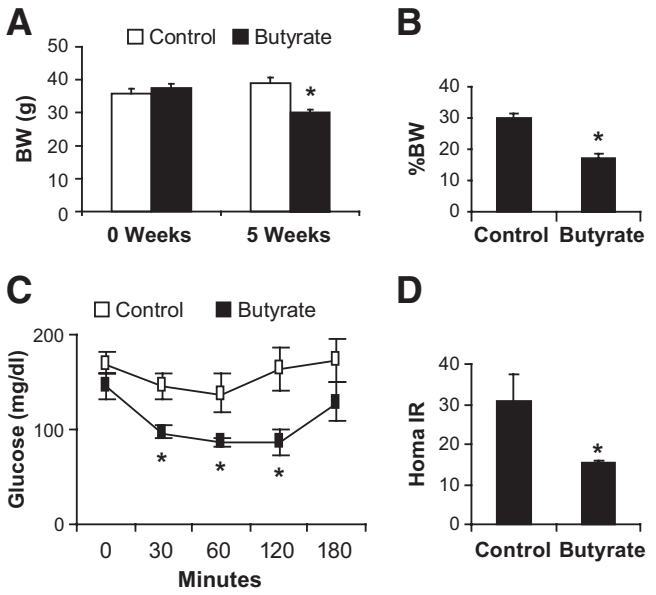

FIG. 7. Treatment of obesity with butyrate. Obesity was induced in C57BL/6J mice fed a high-fat diet for 16 weeks (21 weeks in age). The obese mice were then treated with butyrate through food supplementation for 5 weeks. *A*: Body weight (BW). Body weight was shown at the beginning and end of the 5-week butyrate treatment. *B*: Fat content. Fat content was determined in the body using nuclear magnetic resonance at the end of the 5-week treatment with butyrate. *C*: Intraperitoneal insulin tolerance. At the end of 5 weeks, intraperitoneal insulin tolerance testing was performed after a 4-h fast. *D*: HOMA-IR. Values are the means ± SE (n = 8 in each group). *$P < 0.05$.

increased in both mRNA and protein. The protein elevation was observed in brown fat, skeletal muscle, and liver in butyrate-treated mice. It may be a result of increased mRNA expression or extended half-life of the PGC-1α protein. The change in protein stability is supported by the activities of AMPK and p38 in tissues and cells after butyrate treatment. These kinases phosphorylate the PGC-1α protein and inhibit its degradation (27,28,31–34). As a transcriptional coactivator, PGC-1α transcription activity may be induced by phosphorylation, which leads to removal of a suppressor protein (p160 myb) that is associated with PGC-1α in the basal condition (35). P38 acts downstream of AMPK in the phosphorylation of PGC-1α (36). Therefore, AMPK may increase PGC-1α phosphorylation through direct and indirect (p38) mechanisms. It is not clear how AMPK is activated by butyrate. Butyrate may act through induction of AMP levels in cells from increased consumption of ATP. It was reported that butyrate increases ATP consumption (37). Induction of PGC-1α activity may be a molecular mechanism by which butyrate stimulates mitochondrial function.

Inhibition of histone deacetylase may contribute to increased mRNA expression of PGC-1α, PPAR-δ, and CPT1b. Histone deacetylase inhibition promotes gene expression through transcriptional activation, which is determined by gene promoter activity. Promoter activation requires histone acetylation, which opens chromatin DNA to the general transcription factors for transcription initiation and mRNA elongation. Histone deacetylase inhibits gene promoter activity through deacetylation of histone proteins. In the presence of butyrate, promoter inhibition is prevented by butyrate suppression of histone deacetylase. Histone deacetylase suppression will enhance histone acetylation. This chromatin modification may occur in the gene promoters for PGC-1α, PPAR-δ, and CPT1b for the upregulation of gene transcription.

Butyrate induces type I fiber differentiation in skeletal muscle. In skeletal muscle cells, inhibition of histone deacetylase enhances myotube differentiation in vitro (28–30) and protects muscle from dystrophy in vivo (29–31). In transgenic mice, knockout of class II histone deacetylases was shown to promote differentiation of type I (oxidative) fibers in skeletal muscle (32). This is consistent with our data that type I fiber was increased by butyrate, which inhibits histone deacetylase activities in the skeletal muscle of butyrate-treated mice. TSA, a typical histone deacetylase inhibitor, was tested in parallel treatment with butyrate. TSA exhibited activity similar to that of butyrate in mice (Supplement 2). TSA prevented dietary obesity, insulin resistance, and increased the type I fiber in the skeletal muscle. The activity was associated with elevation of PGC-1α protein. The current study suggests that the metabolic activities of butyrate may be dependent on the inhibition of histone deacetylase.

In summary, dietary supplementation of butyrate can prevent and treat diet-induced obesity and insulin resistance in mouse models of obesity. These activities of butyrate are similar to those of resveratrol (1,2). The mechanism of butyrate action is related to promotion of energy expenditure and induction of mitochondrial function. Stimulation of PGC-1α activity may be a molecular mechanism of butyrate activity. Activation of AMPK and inhibition of histone deacetylases may contribute to the PGC-1α regulation. Butyrate and its derivatives may have potential application in the prevention and treatment of metabolic syndrome in humans.

ACKNOWLEDGMENTS

This study was supported by National Institutes of Health grants DK68036 and P50AT02776-020002 (to J.Y.), American Diabetes Association (ADA) Research Award 7-07-RA-189 (to J.Y.), a pilot grant from the Functional Food Division at the Pennington Biomedical Research Center, ADA Junior Faculty Award 1-09-JF-17 (to Z.G.), and CNRU Grant 1P30 DK072476 sponsored by the NIDDK.

No potential conflicts of interest relevant to this article were reported.

We thank Zhong Wang, Can Pang, Jong-Seop Rim, Qing He, Ms. Xin Ye, and Wei Tseng for their excellent technical support. We thank Thomas Gettys for the antibodies to PGC-1α and UCP-1.

REFERENCES

1. Lagouge M, Argmann C, Gerhart-Hines Z, Meziane H, Lerin C, Daussin F, Messadeq N, Milne J, Lambert P, Elliott P, Geny B, Laakso M, Puigserver P, Auwerx J: Resveratrol improves mitochondrial function and protects against metabolic disease by activating SIRT1 and PGC-1alpha. Cell 2006;127:1109–1122
2. Baur JA, Pearson KJ, Price NL, Jamieson HA, Lerin C, Kalra A, Prabhu VV, Allard JS, Lopez-Lluch G, Lewis K, Pistell PJ, Poosala S, Becker KG, Boss O, Gwinn D, Wang M, Ramaswamy S, Fishbein KW, Spencer RG, Lakatta EG, Le Couteur D, Shaw RJ, Navas P, Puigserver P, Ingram DK, de Cabo R, Sinclair DA. Resveratrol improves health and survival of mice on a high-calorie diet. Nature 2006;444:337–342
3. Watanabe M, Houten SM, Mataki C, Christoffolete MA, Kim BW, Sato H, Messaddeq N, Harney JW, Ezaki O, Kodama T, Schoonjans K, Bianco AC, Auwerx J. Bile acids induce energy expenditure by promoting intracellular thyroid hormone activation. Nature 2006;439:484–489
4.. Zhang CY, Parton LE, Ye CP, Krauss S, Shen R, Lin CT, Porco JA Jr, Lowell BB. Genipin inhibits UCP2-mediated proton leak and acutely reverses obesity- and high glucose-induced beta cell dysfunction in isolated pancreatic islets. Cell Metab 2006;3:417–427

5. Pryde SE, Duncan SH, Hold GL, Stewart CS, Flint HJ. The microbiology of butyrate formation in the human colon. FEMS Microbiol Lett 2002;217: 133–139
6. Roy CC, Kien CL, Bouthillier L, Levy E. Short-chain fatty acids: ready for prime time? Nutr Clin Pract 2006;21:351–366
7. Davie JR: Inhibition of histone deacetylase activity by butyrate. J Nutr 2003;133:2485S–2493S
8. Lin J, Handschin C, Spiegelman BM. Metabolic control through the PGC-1 family of transcription coactivators. Cell Metab 2005;1:361–370
9. Lin J, Wu H, Tarr PT, Zhang CY, Wu Z, Boss O, Michael LF, Puigserver P, Isotani E, Olson EN, Lowell BB, Bassel-Duby R, Spiegelman BM. Transcriptional co-activator PGC-1 alpha drives the formation of slow-twitch muscle fibres. Nature 2002;418:797–801
10. Puigserver P, Wu Z, Park CW, Graves R, Wright M, Spiegelman BM. A cold-inducible coactivator of nuclear receptors linked to adaptive thermogenesis. Cell 1998;92:829–839
11. Mootha VK, Handschin C, Arlow D, Xie X, St Pierre J, Sihag S, Yang W, Altshuler D, Puigserver P, Patterson N, Willy PJ, Schulman IG, Heyman RA, Lander ES, Spiegelman BM. Erralpha and Gabpa/b specify PGC-1alpha-dependent oxidative phosphorylation gene expression that is altered in diabetic muscle. Proc Natl Acad Sci U S A 2004;101:6570–6575
12. Mootha VK, Lindgren CM, Eriksson KF, Subramanian A, Sihag S, Lehar J, Puigserver P, Carlsson E, Ridderstrale M, Laurila E, Houstis N, Daly MJ, Patterson N, Mesirov JP, Golub TR, Tamayo P, Spiegelman B, Lander ES, Hirschhorn JN, Altshuler D, Groop LC. PGC-1alpha-responsive genes involved in oxidative phosphorylation are coordinately downregulated in human diabetes. Nat Genet 2003;34:267–273
13. Petersen KF, Befroy D, Dufour S, Dziura J, Ariyan C, Rothman DL, DiPietro L, Cline GW, Shulman GI. Mitochondrial dysfunction in the elderly: possible role in insulin resistance. Science 2003;300:1140–1142
14. Patti ME, Butte AJ, Crunkhorn S, Cusi K, Berria R, Kashyap S, Miyazaki Y, Kohane I, Costello M, Saccone R, Landaker EJ, Goldfine AB, Mun E, DeFronzo R, Finlayson J, Kahn CR, Mandarino LJ. Coordinated reduction of genes of oxidative metabolism in humans with insulin resistance and diabetes: potential role of PGC1 and NRF1. Proc Natl Acad Sci U S A 2003;100:8466–8471
15. Gao Z, Wang Z, Zhang X, Butler AA, Zuberi A, Gawronska-Kozak B, Lefevre M, York D, Ravussin E, Berthoud HR, McGuinness O, Cefalu WT, Ye J. Inactivation of PKC{theta} leads to increased susceptibility to obesity and dietary insulin resistance in mice.. Am J Physiol Endocrinol Metab 2007;292:E84–E91
16. Ye J, Gao Z, Yin J, He H. Hypoxia is a potential risk factor for chronic inflammation and adiponectin reduction in adipose tissue of ob/ob and dietary obese mice. Am J Physiol Endocrinol Metab 2007;293:E1118–E1128
17. Ye J, Cippitelli M, Dorman L, Ortaldo JR, Young HA. The nuclear factor YY1 suppresses the human gamma interferon promoter through two mechanisms: inhibition of AP1 binding and activation of a silencer element. Mol Cell Biol 1996;16:4744–4753
18. O'Fallon JV, Busboom JR, Nelson ML, Gaskins CT. A direct method for fatty acid methyl ester synthesis: application to wet meat tissues, oils, and feedstuffs. J Anim Sci 2007;85:1511–1521
19. Schwarz M, Lund EG, Setchell KD, Kayden HJ, Zerwekh JE, Bjorkhem I, Herz J, Russell DW. Disruption of cholesterol 7alpha-hydroxylase gene in mice. II. Bile acid deficiency is overcome by induction of oxysterol 7alpha-hydroxylase. J Biol Chem 1996;271:18024–18031
20. Rothwell NJ, Stock MJ. A role for brown adipose tissue in diet-induced thermogenesis. Nature 1979;281:31–35
21. Brooks SL, Rothwell NJ, Stock MJ, Goodbody AE, Trayhurn P. Increased proton conductance pathway in brown adipose tissue mitochondria of rats exhibiting diet-induced thermogenesis. Nature 1980;286:274–276
22. Glick Z, Teague RJ, Bray GA. Brown adipose tissue: thermic response increased by a single low protein, high carbohydrate meal. Science 1981;213:1125–1127
23. Jung RT, Shetty PS, James WP, Barrand MA, Callingham BA. Reduced thermogenesis in obesity. Nature 1979;279:322–323
24. Puigserver P, Spiegelman BM. Peroxisome proliferator-activated receptor-gamma coactivator 1alpha (PGC-1alpha): transcriptional coactivator and metabolic regulator. Endocr Rev 2003;24:78–90
25. Bassel-Duby R, Olson EN. Signaling pathways in skeletal muscle remodeling. Annu Rev Biochem 2006;75:19–37
26. Jager S, Handschin C, St-Pierre J, Spiegelman BM. AMP-activated protein kinase (AMPK) action in skeletal muscle via direct phosphorylation of PGC-1alpha. Proc Natl Acad Sci U S A 2007;104:12017–12022
27. Knutti D, Kressler D, Kralli A. Regulation of the transcriptional coactivator PGC-1 via MAPK-sensitive interaction with a repressor. Proc Natl Acad Sci U S A 2001;98:9713–9718
28. Puigserver P, Rhee J, Lin J, Wu Z, Yoon JC, Zhang CY, Krauss S, Mootha VK, Lowell BB, Spiegelman BM. Cytokine stimulation of energy expenditure through p38 MAP kinase activation of PPARgamma coactivator-1. Mol Cell 2001;8:971–982
29. Wang YX, Lee CH, Tiep S, Yu RT, Ham J, Kang H, Evans RM. Peroxisome-proliferator-activated receptor delta activates fat metabolism to prevent obesity. Cell 2003;113:159–170
30. Sacks FM, Bray GA, Carey VJ, Smith SR, Ryan DH, Anton SD, McManus K, Champagne CM, Bishop LM, Laranjo N, Leboff MS, Rood JC, de Jonge L, Greenway FL, Loria CM, Obarzanek E, Williamson DA. Comparison of weight-loss diets with different compositions of fat, protein, and carbohydrates. N Engl J Med 2009;360:859–873
31. Irrcher I, Adhihetty PJ, Sheehan T, Joseph AM, Hood DA. PPARgamma coactivator-1alpha expression during thyroid hormone- and contractile activity-induced mitochondrial adaptations. Am J Physiol Cell Physiol 2003;284:C1669–C1677
32. Suwa M, Nakano H, Kumagai S. Effects of chronic AICAR treatment on fiber composition, enzyme activity, UCP3, and PGC-1 in rat muscles. J Appl Physiol 2003;95:960–968
33. Terada S, Goto M, Kato M, Kawanaka K, Shimokawa T, Tabata I. Effects of low-intensity prolonged exercise on PGC-1 mRNA expression in rat epitrochlearis muscle. Biochem Biophys Res Commun 2002;296:350–354
34. Zong H, Ren JM, Young LH, Pypaert M, Mu J, Birnbaum MJ, Shulman GI. AMP kinase is required for mitochondrial biogenesis in skeletal muscle in response to chronic energy deprivation. Proc Natl Acad Sci U S A 2002;99:15983–15987
35. Fan M, Rhee J, St-Pierre J, Handschin C, Puigserver P, Lin J, Jaeger S, Erdjument-Bromage H, Tempst P, Spiegelman BM. Suppression of mitochondrial respiration through recruitment of p160 myb binding protein to PGC-1alpha: modulation by p38 MAPK. Genes Dev 2004;18:278–289
36. Xi X, Han J, Zhang J-Z: Stimulation of glucose transport by AMP-activated protein kinase via activation of p38 mitogen-activated protein kinase. J Biol Chem 2001;276:41029–41034
37. Beauvieux MC, Tissier P, Gin H, Canioni P, Gallis JL. Butyrate impairs energy metabolism in isolated perfused liver of fed rats. J Nutr 2001;131: 1986–1992